

Investigation of the Parameters Affecting Subpicosecond Pulse Durations in Passively Mode Locked Dye Lasers

J.-C. Diels, E.W. Van Stryland, and D. Gold

Center for Laser Studies, University of Southern California
Los Angeles, CA 90007, USA

We report the shortest pulses generated to date using a simple dispersionless three mirror cavity. In addition, for the first time, accurate fringe resolved autocorrelation measurements with a peak to background ratio of 8 to 1 are presented. These fringes enable us to determine in a single recording whether or not the pulses are bandwidth limited.

Passive mode locking has been made previously in a dispersive cavity containing either two jets (7 optical elements) or one jet of active medium and one short cell of saturable absorber (8 optical elements in the cavity). The shortest pulse durations measured with these cavities were respectively 0.5ps [1] and 0.3ps [2]. Pulses as short as 0.17ps have been generated using a simple dispersionless cavity of only 4 optical components (2 focusing mirrors and a flat output mirror). The saturable absorbers (dioxadicyanone-iodide or DODCI and malachite green) were mixed with the Rhodamine 6G-ethylene glycol solution in the single jet stream of the laser. There are no prisms, etalons or dye cells which may act as a pulse bandwidth limiting element. After all, dye cells cannot be shortened indefinitely. The shortest pulses were obtained using a mirror having a reflectivity of 99.7% between 600 and 620 nm. Within that range, the dispersive properties of the dye solution select the wavelength.

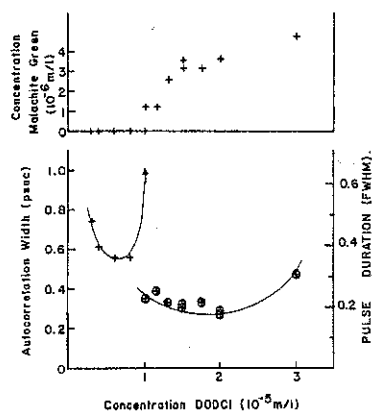


Fig. 1 Concentration dependence of the pulse duration

The dye was excited by cw argon ion laser with stabilized output power (Control Co, model 552). The pulse duration, as measured at threshold by a standard second order autocorrelation method, is plotted in Fig. 1, as a function of the composition of the dye solution. The left ordinate indicates the FWHM of the autocorrelation trace, while the actual pulse duration (FWHM) is shown on the right ordinate. A scale ratio of 1.55 is used, corresponding to

sech² shaped pulses, as justified by autocorrelation fits presented below. The concentration of Rhodamine 6G was 2 X 10⁻² M/l. As DODCI alone is added to the solution, the pulse duration drops rapidly to a minimum. These data points (no malachite green, DODCI concentration X 10⁻⁵ M/l) are extremely dependent on particular cavity configuration and losses. At a concentration of 10⁻⁵ M/l of DODCI, the laser pulses have low coherence and long duration, as observed from the fringe resolved autocorrelation measurement. Good mode locking is restored by the addition of malachite green, the concentration of which is plotted in the upper part of the figure.

To measure pulse durations by second order autocorrelation methods, the pulse train is split into two beams. Both beams are recombined with a known differential delay. They are then sent through a frequency doubling crystal. The signal recorded is the second harmonic pulse energy as function of the delay between trains. All the methods used differ in the type of nonlinear mixing. In the zero background methods [3], one detects the product of both fields, while for methods including background [2], the fields of both pulse trains are added. If $E(t) = \mathcal{E}(t)\cos(\omega t + \phi t)$ is the electric field of a light pulse, the function of delay measured by the latter method is the time average:

$$\int |E(t) + E(t-\tau)|^2 dt = 3/8 \int (\underline{\mathcal{E}^4(t)} + \underline{\mathcal{E}^4(t-\tau)} + 4\underline{\mathcal{E}^2(t)\mathcal{E}^2(t-\tau)} + 4[\mathcal{E}^2(t) + \mathcal{E}^2(t-\tau)] \mathcal{E}(t)\mathcal{E}(t-\tau) \cos[\omega\tau - \phi(t) + \phi(t-\tau)] + 2\mathcal{E}^2(t)\mathcal{E}^2(t-\tau) \cos 2[\omega\tau - \phi(t) + \phi(t-\tau)]) dt \quad (1)$$

Only the underlined terms are measured in conventional techniques, which average out the fast variations at $\cos\omega\tau$ and $\cos 2\omega\tau$. The first two terms are constant factors independent of pulse overlap, and give a contribution of $2\int \mathcal{E}^4 dt$ in the wings of the autocorrelation trace. With the next term, (which is the only one measured in "zero background" methods) the autocorrelation function peaks at $6\int \mathcal{E}^4 dt$ in the center of the trace ($\tau=0$), giving the standard peak to background ratio of three to one. We have constructed an accurate autocorrelator that is able to

resolve the next interference terms, which are the only ones that contain phase information. The contributions of all terms at $\tau=0$ add up to $16\int \mathcal{E}^4 dt$, yielding a peak to background ratio of eight to one, which is exactly what was observed. A sample of an experimental recording near the center of the trace is shown in Fig. 2. The solid line is the experimental recording while the circles indicate the functional fitting of (1), assuming the phase factor is constant within the range. While the sample

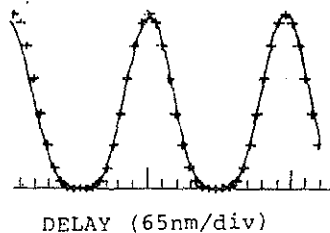


Fig. 2

of Fig. 2 covers only a delay of two light periods, our measurements scan continuously across the full autocorrelation width.

The advantage of recording the full autocorrelation function including the fast variation is that we keep phase or frequency information that is otherwise lost. Figure 3 shows a numerical

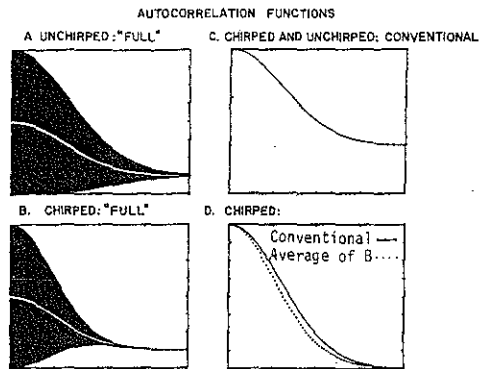


Fig. 3

comparison of the full autocorrelation traces (a and b) and conventional (c) for unchirped (a) against chirped (b) pulses. Figure 3c is the same for chirped and unchirped pulses. The pulses are gaussian shaped ($\xi(t) = \exp\{-(t/W)^2\}$) with a linear chirp $\phi(t) = a(t/W)^2$. Even though the chirp is very small ($a=0.16$), its presence can be inferred at once from the shape of the corresponding autocorrelation curve. A quantitative study of the phase content of the pulse can be made by comparing the curve obtained by taking the average of the maximas and minimas of the complete autocorrelation function (white line in Fig. 3a and b) to the conventional autocorrelation. Such a comparison, with backgrounds subtracted and renormalized, is shown in Fig. 3d. From (1), it can be seen that the average (with background subtracted) has the shape $\int dt \xi^2(t) \xi^2(t-\tau) \{1 + \frac{1}{2} \cos 2[\phi(t) - \phi(t-\tau)]\}$. When the phases are constant, this expression has the same shape as the zero background autocorrelation function.

An experimental comparison is made in Fig. 4. On the upper left corner of Fig. 4, a full experimental recording of the complete autocorrelation function is shown (only the envelope of the maximas and minimas of the interferences is shown). Note that the peak to background ratio is exactly eight to one. The energy average of that measurement shown in the upper right corner is the conventional autocorrelation measurement, with peak to background ratio of exactly 3. The solid line is the experimental recording, while the crosses are a fit to the autocorrelation of a superposition of two sech shaped (amplitude of the electric field (+) pulses. The shorter pulse has a width of 0.19ps and contributes to the central portion of the trace. The broader pulse only contributes to the wings of the autocorrelation function.

The 3/1 autocorrelation experimental curve is retraced on the bottom of Fig. 4 (solid line), and compared to the average of the top and bottom traces of the full autocorrelation measurement (dashed line). The fact that both curves are different, indicates that our signal is not pure in phase. Analysis of oscilloscope traces, pulse spectrum and autocorrelation measurements indicate that the pulse train oscillates regularly between two different regimes. Thus, the two sech pulses of

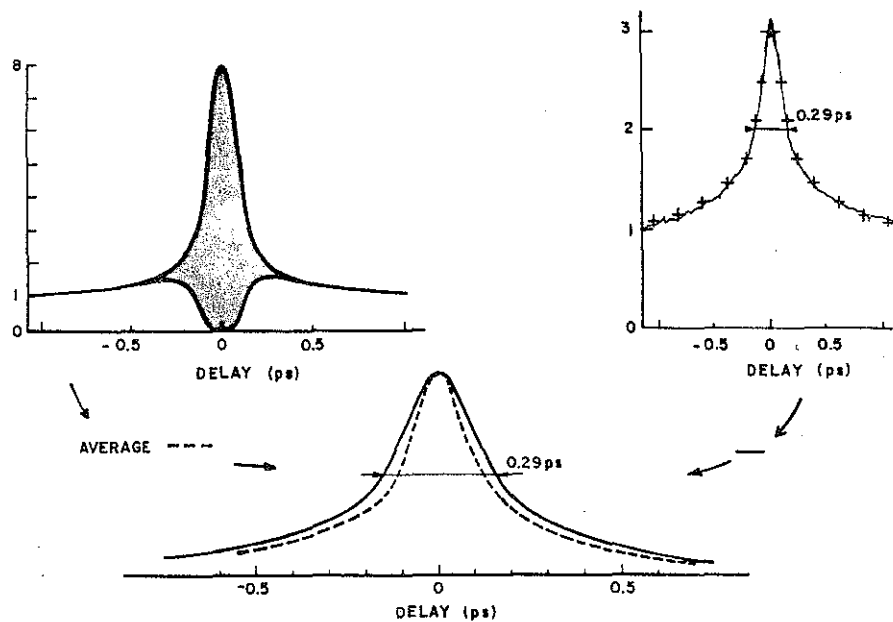


Fig. 4

the aforementioned fit have different frequencies. Measurements indicate that closest to threshold, we have the narrowest pulses centered at 615 nm. As the pump slightly increases, the pulses broaden while the average frequency shifts upward.

It should be noted that the autocorrelator, being made of BK7 glass, does affect the measurement itself. According to linear dispersion theory, [4] a measured pulse of 0.19ps FWHM had a width of 0.17ps before entering the interferometer.

References

1. C.V. Shank, E.P. Ippen: Appl. Phys. Lett 24, 373 (1974).
2. I.S. Ruddock, D.J. Bradley: Appl. Phys. Lett. 29, 296 (1976).
3. E.P. Ippen and C.V. Shank, Appl. Phys. Lett. 27, 488 (1975).
4. D. von der Linde, Appl. Phys. 2, 281 (1973).

Work supported by NSS, number ENG 76-06231.